Effect of nonsuperconducting secondary inclusions on the magnetization relaxation in melt-processed $R\mathrm{Ba_2Cu_3O_{7-\delta}}$ (R=Nd and Yb) bulk superconductors at high temperatures

Tadashi Mochida, Noriko Chikumoto, and Masato Murakami
Superconductivity Research Laboratory, International Superconductivity Technology Center, 1-16-25, Shibaura, Minato-ku, Tokyo 105-0023, Japan

(Received 29 June 2000; revised manuscript received 30 October 2000; published 24 July 2001)

We have studied the effect of nonsuperconducting inclusions on the magnetization relaxation in melt-processed $R\mathrm{Ba_2Cu_3O_{7-\delta}}$ (R=Nd and Yb) bulk superconductor in a high-temperature region ($77 \leqslant T \leqslant 90$ K). It is found that nonsuperconducting inclusions are mainly effective in reducing the normalized relaxation rate S ($\equiv -d \ln M/d \ln t$) at low fields [$b_{irr}(\equiv \mu_0 H_a / B_{irr}) \lesssim 0.1$] and at high fields ($b_{irr} \gtrsim 0.4$). A suppression in S is observed in an intermediate field region ($0.1 \lesssim b_{irr} \lesssim 0.4$) for the samples exhibiting secondary peak effect, suggesting a relation between the peak and the suppression.

DOI: 10.1103/PhysRevB.64.064518 PACS number(s): 74.60.Ec, 74.60.Ge, 74.60.Jg

I. INTRODUCTION

Flux creep measurements are informative for understanding flux pinning behavior of irreversible type-II superconducting materials.[1,2] However, a data analysis of magnetic relaxation has several difficult problems to overcome. First, one cannot measure ''true'' critical current density (J_{c0}), which is the current density based on the critical state model without any relaxation. J_{c0} is difficult to measure due to the fact that relaxation always takes place until one reaches the starting point or the target field (B) and temperature (T). In other words, when one reaches an empirical starting point, the critical state of the superconductor is already relaxed. Another important parameter of ''true'' pinning energy (U_0) is not available, because the J window, which can be measured in flux creep measurements under constant B and T, is too small to gather any reliable data to deduce U_0. Maley *et al.*[3] have used an effective method to obtain a U-J relationship in a wide J window. However, since several data at different temperatures are used to draw a single U-J curve, fitting parameters are employed. Hence absolute values of J_{c0} or U_0 cannot be obtained with this method. Here one should bear in mind that critical current density J_c is a nonequilibrium property of type-II superconductors, which inherently makes the handling of J_c, including its technical meaning, extremely difficult.

Despite its intrinsic ambiguity, flux creep measurements are highly important for practical applications, since one cannot avoid the effect of thermal activation. Hence, instead of using J_{c0}, it is practical to use a so-called apparent current density, which is the current density that the superconductor can carry without resistance after some relaxation time. For engineering applications, it is common to employ some electric-field criterion (typically 10^{-6} V/m) for the determination of practical J_c value, which is used for the design of the superconducting magnet system. In both high and low T_c materials, it is known that J decays logarithmically with time if the pinning force is sufficiently high. In this case, since the time decay is logarithmic, one can easily set a practical J_c value with taking account of the safety margin for engineering applications. It is also possible to use the flux creep data in understanding flux pinning behavior. Furthermore, since one can see semidynamic properties of flux lines with flux creep measurements, it might be useful to study a difference in the pinning mechanism. On the other hand, nonlogarithmic decay of J is often observed in weakly pinned materials like Bi-Sr-Ca-Cu-O,[4] for which the apparent current density cannot be used either for practical J_c or pinning characterization.

Melt-processed $R\mathrm{Ba_2Cu_3O_{7-\delta}}$ (R123) bulk superconductors have significant potential for various industrial applications, since they exhibit large J and high irreversibility field (B_{irr}) even at elevated temperatures. This is due to the fact that they contain finely distributed $R_2\mathrm{BaCuO_5}$ (or $R_4\mathrm{Ba_2Cu_2O_{10}}$) nonsuperconducting secondary inclusions, which can act as ''strong'' pinning centers particularly in a low-field region.[5] Recently another possible ''strong'' pinning center, which is active at elevated temperatures, was found in R123. When R123 (R=Nd, Sm, Eu, Gd) is melt processed in a reduced oxygen atmosphere, R-rich $R_{1+x}\mathrm{Ba_{2-x}Cu_2O_{7-\delta}}$ clusters ($R123ss$) about 10–100 nm are distributed in near stoichiometric R123 matrix, which are supposed to provide additional strong pinning.[6,7] Koblischka *et al.*[8] reported that the $R123ss$ clusters with depressed T_c are responsible for field-induced pinning, which leads to the secondary peak effect or the ''fishtail,'' and thus J_c enhancement at intermediate fields.

In the former study,[9] we systematically studied the effect of nonsuperconducting $\mathrm{Nd_4Ba_2Cu_2O_{10}}$ (Nd422) secondary inclusions on J in Nd123 samples prepared by the oxygen-controlled melt-growth (OCMG) process,[6,7] and found that Nd422 and Nd123ss can simultaneously contribute to pinning enhancement, in that overall J is almost a simple summation of these two contributions. Although both Nd422 and Nd123ss are strong pinning centers, the energy for a single vortex interaction can be different due to a large difference in their size. Nd422 inclusions of 0.1–2 μm diameter would have much deeper pinning potential than weakly superconducting Nd123ss of 10–100 nm (whereas the density of Nd422 is much lower than that of Nd123ss). It is thus interesting to study how Nd422 inclusions affect the relaxation

TABLE I. The list of the *R*-Ba-Cu-O samples used in this study.

Sample	T_c (K) onset	V_f	d $\times 10^{-6}$ m	V_f/d $\times 10^{5}$ m^{-1}	$1-(6/5)V_f$
FSC	93.8	0.00		0.0	1.00
MT1	94.5	0.19	1.9	1.0	0.77
MT1F	94.5	0.18	1.2	1.5	0.78
MT2	94.5	0.25	1.8	1.4	0.70
MT3	95.0	0.34	1.7	2.0	0.59
Yb1.8	88.5	0.23	1.1	2.1	0.72

rate (S), especially when the pinning by Nd123*ss* is simultaneously in function.

In this study, we investigated the effect of Nd422 on the magnetization relaxation by using various Nd123 samples with different sizes and amounts of Nd422. We also measured magnetic relaxation of a melt-textured Yb123 sample which did not exhibit ''fishtail'' for comparison.

II. EXPERIMENT

Table I is the list of the samples studied in the present experiment. A Nd123 single crystal (sample FSC) was grown with a flux method in flowing 0.1% O_2/Ar mixture gas, the details of which are described in Ref. 10. OCMG processed Nd123 samples, with different sizes and amounts of Nd422, were prepared in flowing 0.1% O_2/Ar mixture gas. Here, V_f and d are the volume fraction and the average diameter of Nd422. The value of V_f/d, which is proportional to the surface area of secondary inclusions, is known as an index representing the pinning parameter in melt-processed Y123 samples.[5] It is notable that V_f values are comparable between MT1 and MT1F, while d for MT1F is drastically reduced to 1.2 μm. d values are similar among MT1, MT2, MT3, while V_f values are varied from 0.19 to 0.34. Therefore the effect of Nd422 refinement can be studied by comparing between MT1 and MT1F, while that of Nd422 content by MT1, MT2, and MT3. The details of sample preparation for MT1, MT2, and MT3 are described in the Ref. 11 while that for MT1F is in the Ref. 12. Bulk Yb123 sample (sample Yb1.8) was prepared with a conventional melt processing in air, the details of which are described elsewhere.[13,14] All the samples showed a sharp superconducting transition width <2 K, which demonstrates that the sample quality is sufficiently good for fair comparison. The details of *J*-*B* properties and irreversibility lines for Nd-based samples and Yb1.8 are described in the Refs. 9 and 14, respectively.

Magnetization measurements were carried out using a Quantum Design superconducting quantum interference device (SQUID) magnetometer (MPMS-7) with magnetic fields applied parallel to the *c* axis. Measurements were performed in a persistent current mode with a scan length of 30 mm, which is widely used in many studies.[3,15–18] In this condition, the field inhomogeneity was less than 0.01%. The apparent current density was deduced from the irreversibility magnetization using the extended Bean model[19] with the relation $J=20\Delta M/a(1-a/3b)$, where J is in A/m^2, ΔM is the irreversible magnetization in emu/m^3, and a and b ($a>b$) are cross-sectional dimensions in m perpendicular to the field. Magnetic relaxation was measured in a normal dc mode by monitoring the time decay of magnetic moment. For relaxation measurements, the magnetic field was swept to a sufficiently low negative value to ensure full flux penetration, and then set to the target value. The data were taken every 60 s for 50 min, which is reported to be long enough to deduce flux creep properties.[18] The normalized relaxation rate (S) is given by

$$S(t) \equiv -d \ln M(t)/d \ln t. \tag{1}$$

we deduced an S value *directly* from the slope of a ln$M$-ln$t$ plot. Here, data at $t>500$ s were used to avoid the effect of field sweep rate. An S value calculated using the data at $500<t<1500$ s is denoted as S_{I} while that at $t>1500$ s is S_{II}, respectively. Since the plots are almost linear in the measurement time range, we regressed the slope linearly using a least-square method. We defined $t=0$ as the time when the first data were acquired. Here, there was a certain time delay (t_{delay}) before starting the first data acquisition after the field had reached the target value. If t_{delay} is large, the error in S (denoted as ΔS) cannot be neglected. Our observation confirmed that the t_{delay} was <10 s, and hence ΔS caused by this delay was well below 1.2% as long as the data at $t>500$ s were used. Even if $t_{delay}\simeq 50$ s, which is much longer than the observed t_{delay} value, ΔS is within 6%. When S values were calculated using data at $t>1500$ s, ΔS is less than 2.4% even if t_{delay} is of the order of 50 s.

III. RESULTS AND DISCUSSION

In the set of samples with various amounts of nonsuperconducting inclusions, it is evident that cross-sectional area of superconducting matrix decreases by adding nonsuperconducting inclusions. Since Nd422 inclusions are much larger than the size of coherence length, Nd422 addition will result in a depression in the apparent supercurrent even when the net critical current density (J_{net}) is identical. Thus we deal with J_{net} flowing in the superconducting matrix, together with the apparent current density, taking account of a decrease in the supercondcting matrix. For this purpose, we employ the bond-percolation model,[20] which is used to deduce the net current in a composite material. According to the model, current flowing in a superconductor decreases by factor of $P=(x-x_c)/(1-x_c)$, where $x=(1-V_f)$ is the ratio of superconducting phase, $x_c\equiv 2/N$ the critical density, and N the bond number. Using $N=12$ as the densest case, the apparent (observed) J is given by $J\equiv PJ_{net}=\{1-(6/5)V_f\}J_{net}$.

Figure 1 shows the field dependence of the J_{net}. The error bar stands for the local magnetic induction ΔB, which reflects nonuniform distribution of B within the sample and thus is dependent on both J and the sample size. A secondary peak effect is observed in all the samples except for Yb1.8

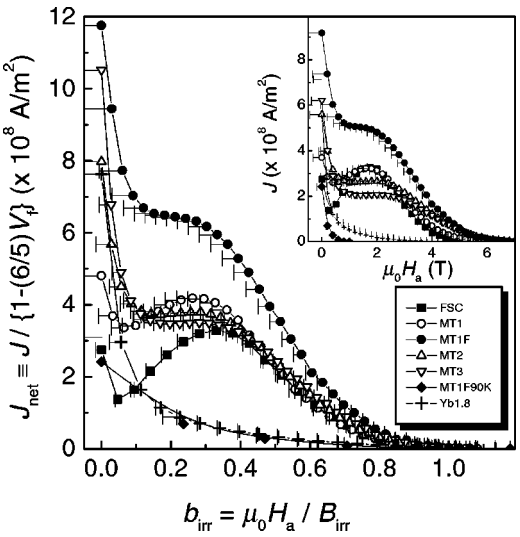

FIG. 1. Plots of $J_{net}(\equiv J/\{1-(6/5)V_f\})$ versus $\mu_0 H_a / B_{irr}(\equiv b_{irr})$ at 77 K with the applied field parallel to the c axis for the samples studied here. Inset shows J plotted against $\mu_0 H_a$. The error bar stands for the field variation caused by the local magnetic induction, which is estimated from J and the sample size.

and MT1F at 90 K. FSC shows small J_{net} values in a low-field region with a pronounced peak effect. By contrast, the sample MT3, which has the largest V_f and V_f/d values, shows large J_{net} values in a low-field region, with a rather smeared peak on the shoulder. The magnitude of the peak for MT2 lies in between MT1 and MT3. MT1F shows the largest J_{net} values at all the fields, because fine Nd422 inclusions can act as effective pinning centers in the entire field region.[9] Neither Yb1.8 nor MT1F at 90 K has the secondary peak effect, which is similar to well-oxygenated melt-processed Y123 sample.[21] Koblischka *et al.*[22] suggested that *R*123*ss* has T_c of around 88 K, and can provide a fluctuation in T_c below this temperature, based on the observation of two-step superconducting transition in the field-cooled curve. It is thus understandable that no peak is observed in MT1F at 90 K. It is also reasonable that the secondary peak is not observed in Yb1.8 at all temperatures, since no fluctuation in T_c is present in well-oxygenated Yb123.

Typical magnetic relaxation signals for MT1F and Yb1.8 are shown in Fig. 2. Solid symbols are the plots with $t_{delay}=0$ s, while open symbols are for $t_{delay}=50$ s. One should note several features which will be the important points in the following discussions. First, the magnetization signals are much larger than the absolute sensitivity of the SQUID (10^{-6} emu). Smooth data means the error (or the standard deviation) of differential sensitivity is sufficiently small in comparison with the order of the decay of magnetization. These results provide confirmations that the signals are large enough to deduce reliable S values. Second, t_{delay} does not cause any significant difference in S values which were calculated using the data at $t>1500$ s. Third, an almost pure logarithmic M-ln$t$ relation indicates that the U-J relation is almost linear in the experimental time window.

Generally speaking, the S value is dependent on the height of the effective pinning barrier (U). A difference in the relaxation behavior has well been described in terms of a current dependency of the pinning potential $U(J)$, in that $U(J)$ is given by the following inverse power-law form:[15]

$$U(J)=(U_c/\mu)[(J_{c0}/J)^{\mu}-1], \tag{2}$$

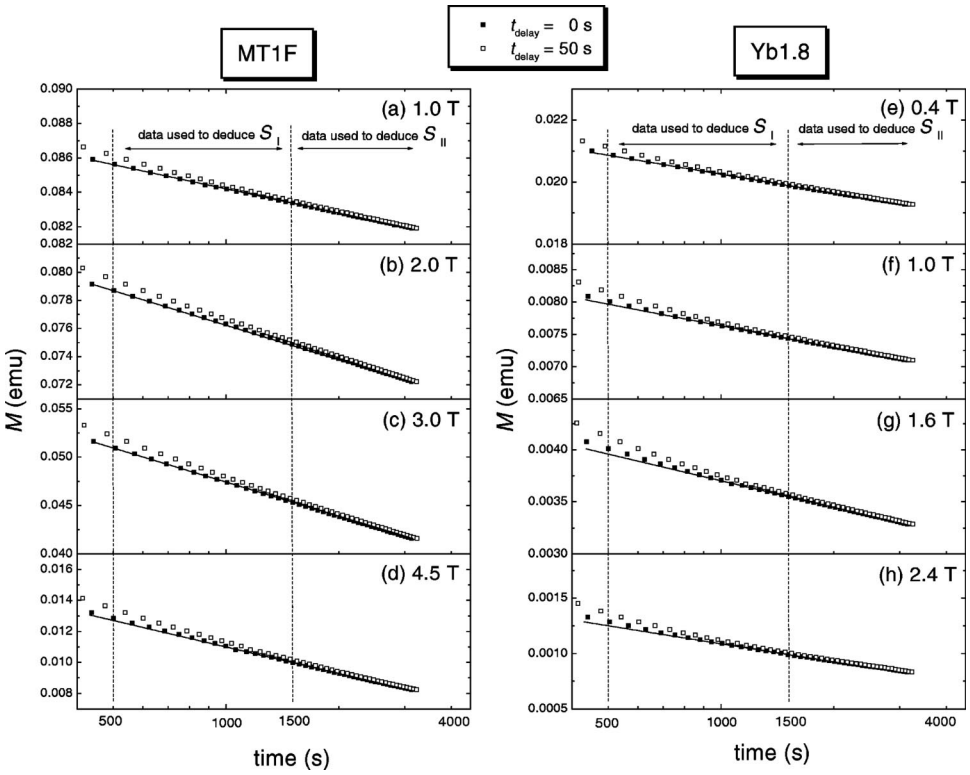

FIG. 2. The magnetic relaxation data at 77 K for MT1F at (a) 1.0 T, (b) 2.0 T, (c) 3.0 T, (d) 4.5 T, and for Yb1.8 at (e) 0.4 T, (f) 1.0 T, (g) 1.6 T, and (h) 2.4 T, showing typical results. The filled square is the plot with delay time $t_{delay}=0$ s (as measured) whereas open square is the case of $t_{delay}=50$ s. Data at $500<t\leqslant 1500$ s and 1500 s$<t$ are used to deduce S_{I} and S_{II}, respectively. The solid line is the slope for the data at $t>1500$ s with $t_{delay}=0$ s. No significant difference is found in the slope between $t_{delay}=0$ and 50 at $t>1500$ s. Note that the resolution of the measurements is sufficient to deduce the reliable slope S.

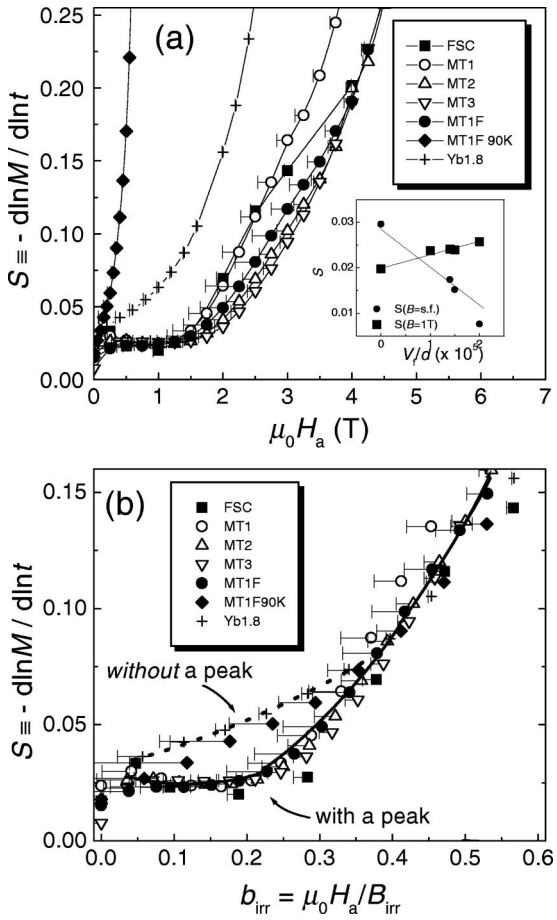

FIG. 3. Field dependence of S_{II} for the samples at 77 K are plotted versus (a) applied field $\mu_0 H_a$ and (b) reduced field $b_{irr}(\equiv \mu_0 H_a / B_{irr})$. Data for MT1F at 90 K are also plotted. The lines are guides for eyes.

where U_c is the characteristic pinning energy, U the height of energy barrier at J, and μ the glassy exponent that reflects how the energy barrier grows with decreasing J. Here, one should note that the ratio J/J_{c0} is larger at larger values of J, and the activation barrier $U(J/J_{c0})$ is smaller. The current dependence of S is especially important at elevated temperatures where a large relaxation in J takes place.

In the following, we will describe the effect of Nd422 inclusions on the magnetic relaxation both on S and S-J relation. The S-$\mu_0 H_a$ curves for the Nd-based samples are shown in Fig. 3(a), in which S_{II} is plotted as S. Note that ΔS is smaller than the size of symbol mark. In general, S is small and relatively field independent at low fields, however, it grows rapidly at higher fields. At low fields, some compositional dependence is recognized although S value is almost field independent. The inset of Fig. 3(a) shows the relation between V_f/d and S. In the remnant state, S for MT3 is the smallest ($S=0.76\times10^{-2}$), while that for FSC is the largest ($S=3.0\times10^{-2}$), i.e., S is found to be small for the sample with large V_f/d value. At $\mu_0 H_a=1.0$ T, however, S for FSC is the smallest ($S=2.0\times10^{-2}$) while that for MT3 is the largest ($S=2.6\times10^{-2}$), i.e., S is the smaller for the sample with the larger V_f/d value. When magnetic field exceeds 1.5 T, S grows rapidly with field, in that strong sample dependence is observed. An increase in S is the most prominent for FSC, whereas it is small for the samples with large V_f/d values. These results indicate that Nd422 inclusions are effective in reducing S in low and high fields. It is evident that the field dependence of S is similar among the Nd-based samples in spite of their large difference in the shape of J_{net}-$\mu_0 H_a$ curve. This may indicate that the J_{net}-$\mu_0 H_a$ curve is not directly related to the field dependence of S.

The relation between S and the peak effect is an interesting subject. Here we will study it using the data for Yb1.8 at 77 K and MT1F at 90 K as the samples without the peak effect. However, fair comparison is difficult since B_{irr} values differ significantly among the samples. Thus, a scaling procedure would be useful. Here, a scaling using the upper critical field B_{c2} would be a more common procedure. However, it is very difficult to deduce the B_{c2} value in the materials studied here. On the other hand, it is known that B_{irr} is a useful parameter that enables an empirical scaling in $R123$,[8,16,23] which will lead to a practical comparison. Although a scaling using magnetic induction that gives the maximum J_c (so-called a peak field B_{pk}) is also useful for empirical comparison, B_{pk} is known to have a close relation with B_{irr}.[24,25] Therefore, in this study, we used B_{irr} for normalizing the field.

Figure 3(b) shows the $b_{irr}(\equiv \mu_0 H_a / B_{irr})$ dependence of S for the Nd- and Yb-based samples, to study the relation between S-b_{irr} and a peak, by comparing the samples with and without a peak in J (or J_{net}). It is clearly recognized that samples with a peak exhibit a depression in S at $0.1 \lesssim b_{irr} \lesssim 0.4$, where J enhancement with a peak is observed. In addition, S value for MT1F at $0.1 \lesssim b_{irr} \lesssim 0.4$ is increased when temperature is raised from 77 to 90 K, as the peak in J-$\mu_0 H_a$ curve smears.[9] These results suggest that a reduction in S is closely correlated with the peak in J.

On the other hand, S at $b_{irr} \gtrsim 0.4$ is not affected by the presence of the secondary peak effect. This shows that the pinning mechanism causing a peak in J is different from the one that determines S at $b_{irr} \gtrsim 0.4$. It is important to note that S-b_{irr} curves for the Nd-based samples are almost identical, regardless of the fact that S-$\mu_0 H_a$ curves at high fields is reduced by Nd422 addition as shown in Fig. 3(a). This indicates a close relation between S and B_{irr}. The higher B_{irr} values for melt-processed samples are thus linked to the suppression in S caused by Nd422 addition.

To further confirm the effect of Nd422 inclusions on S and pinning energy, we studied the current dependency of S. Here, $S_I(J=J_I)$ values were regarded as S at large J, while $S_{II}(J=J_{II})$ as S at smaller J values. The respective J values were determined as $J_I \equiv \{J_{net}(t=500s)+J_{net}(t=1500s)\}/2$ and $J_{II} \equiv \{J_{net}(t=1500s)+J_{net}(t=3000s)\}/2$. The decay of $J[\equiv J(t=3000s)/J(t=500s)]$ at $\mu_0 H_a=1$, 2, and 3 T are found to be about 0.96, 0.92, and 0.82, respectively.

Figure 4 shows the current dependence of S for the Nd-based samples at $\mu_0 H_a=1$, 2, and 3 T, which corresponds to $b_{irr} \approx 0.16 \pm 0.02$, 0.32 ± 0.04, and 0.48 ± 0.06, respectively. It is found that a refinement of Nd422 inclusions (denoted as SI refinement in Fig. 4) led to an enhancement in J_{net} at 1 T. It also affected S-J_{net} relations at 2 and 3 T, i.e., it *reduced*

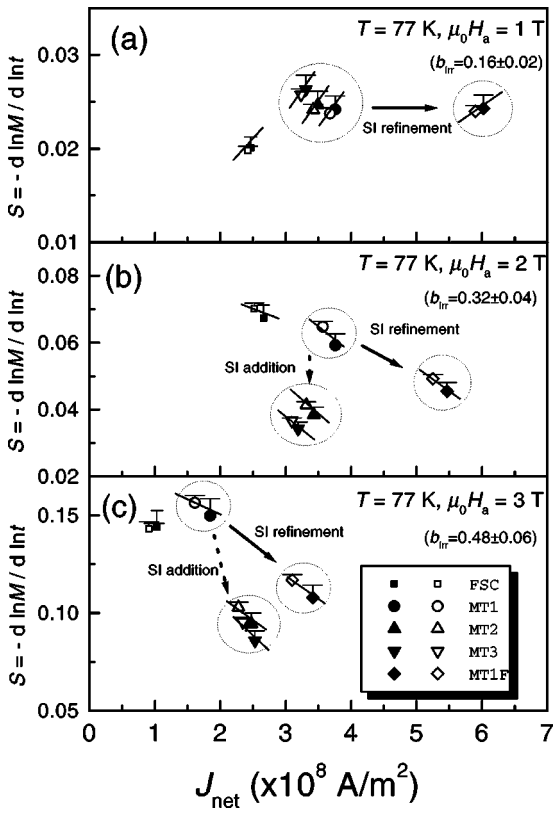

FIG. 4. Plots of $S_{\mathrm{I}} \equiv S(J_{\mathrm{I}})$ (filled symbols) and $S_{\mathrm{II}} \equiv S(J_{\mathrm{II}})$ (open symbols) versus J_{net} at 77 K and at (a) 1 T, (b) 2 T, and (c) 3 T for the Nd-based samples. For the details of the samples, see the experimental and Table I. The circles and arrows are guides for eyes showing the effect of Nd422 (SI refinement and addition) on *S*. The solid lines are guides for eyes showing the effect of SI both on the *S* and *S*-*J* relation.

S with *increasing* J_{net}. This result is important because it reveals the fact that the improvement in the pinning properties by Nd422 refinement is related to the macroscopic pinning force. For example, a symple $S(J_{net})$ can be given as

$$1/S(J_{net}) = U_c[1-(J_{net}/J_{c0})], \tag{3}$$

since *S* is inversely proportional to the height of the energy barrier, and that a linear U-J_{net} relation can be assumed from the experimental result. This means either U_c, J_{c0}, or both are increased by Nd422 refinement. Note that the result is not affected even if a nonlinear dependence is assumed. Thus it is concluded that Nd422 refinement enhances macroscopic pinning force in the entire field region. Similarly, the reduction in *S* by Nd422 addition (denoted as SI addition), presented in Figs. 4(b) and (c), indicates that Nd422 addition is also effective in enhancing the macroscopic pinning force in this field region.

It would be important to see whether the results can be explained in terms of the dynamic mechanism,[26] because it has been controversial whether the differences in *S* can be explained by this mechanism or the macroscopic pinning force. Basically, the dynamic mechanism assumes the ''true'' (unrelaxed) critical current density which monotonously decreases with field. An observed *J* value is interpreted in terms of a difference in *S*, which basically depends on the ratio of J/J_{c0}, i.e., how far the system has relaxed from J_{c0}. Within the scope of the dynamic scenario, a reduction in *S* by Nd422 refinement may be explained in terms of a smaller J_{net}/J_{c0} value. However, our experimental results did not show a J_{net} reduction. Moreover, the Nd422 refinement led to a smaller *S* value and an enhancement in J_{net}, simultaneously. If the dynamic scenario is applied in Eq. (3) to explain a smaller *S* value, it requires either a larger J_{c0} value (to obtain a smaller J_{net}/J_{c0} value) or a larger U_c value. In the former case, a large J_{c0} value means a larger pinning force. In the latter case, an increase in U_c directly means a larger pinning force. These suggest that the differences in *S* among the samples are not attributed to the differences in J_{net}/J_{c0} value alone but to the macroscopic pinning force. Therefore the effect of Nd422 refinement on the *S*-*J* relation cannot be explained within the scope of the dynamic scenario.

It is worthwhile to note that Fig. 4 shows an anomalous *S*-*J* relation common to all the samples at 2 and 3 T in that *S* value is higher for a smaller J_{net}, i.e., $S_{\mathrm{II}} \equiv S(J_{\mathrm{II}}) > S_{\mathrm{I}} \equiv S(J_{\mathrm{I}})$, which is the negative *J* dependence of *S*. This contradiction can be understood as follows. Using the $U(J)$ relation combined with a conventional flux creep theory, *S* is given by[1,2,27]

$$S(t) \equiv kT/[U_c + \mu kT \ln(t/t_{eff})], \tag{4}$$

where t_{eff} is an effective attempting time for vortex motion. Here, we note whether Eq. (4), which is the so-called logarithmic solution, is applicable or not in this study. Recently, Burlachkov *et al.*[28] noted that, when the U-J relation is highly nonlinear, the logarithmic solution may show significant deviations from the exact one, especially at short times. However, in the present study, *U* is found to be almost linear function of *J* in the experimental window. Therefore Eq. (4) is applicable in the present study, even based on the idea of Burlachkov *et al.* Equation (4) indicates that *S* is dependent not only on U_c but also on μ, *t*, and t_{eff}. When a sample is measured under a constant *B* and *T*, it is natural to assume that U_c and t_{eff} are constant. This means that *S* is dependent only on μ and *t*. The fact that *S* increases with *t* thus indicates that μ is *negative* at 2 and 3 T. Figure 4(a) shows normal *S*-*J* relation at 1 T, indicating μ is *positive* at this field. On the other hand, a negative *S*-*J* dependence is found at 77 K and $0.2 \lesssim b_{irr} \lesssim 0.8$, which is the experimental window of the present study, for all the Nd-based samples. This implies that μ is *negative* at $0.2 \lesssim b_{irr} \lesssim 0.8$.

Finally, we will discuss the origin of negative μ. According to the collective-creep (CC) model[29] and vortex glass model,[30] μ is expected to be positive for all the regimes, because the model treats the vortex lattice as an elastic continuum, which interacts with randomly distributed weak pinning centers. However, vortices will not creep collectively when pinning is strong.[31] Therefore magnetic relaxation may not follow the CC model and thus μ can be negative for strongly pinned superconductors like the samples treated here. In fact, negative μ was also observed through transport measurements in a melt-processed Y123 with a peak.[32] In

addition, negative μ is found in various superconductors in a different temperature and field region.[33,34] This suggests that negative μ is related to the extrinsic defect structure and its interaction with vortices. As we have observed in the OCMG-processed Nd-based samples, the crossover in μ from positive to negative takes place at around $b_{irr} \approx 0.2$, where anomalous J enhancement takes place. It is thus probable that negative μ is caused by the interaction between vortices induced by the activation of Nd123*ss*. One scenario is that collective interaction between vortices is destroyed by the activation of Nd123*ss*, since the density of Nd123*ss* is high enough to pin all the vortices at $\mu_0 H_a \leqslant B_{irr}$, in that Kim-Anderson type[35] ($\mu = -1$) flux motion takes place leading to a negative μ value. Another scenario is that plastic interaction between vortices is induced by the activation of Nd123*ss*. The pinning energy associated with a Nd123*ss* interaction is so small that the vortices pinned by Nd123*ss* will be depinned leading to local deformation. It is interesting that Abulafia *et al.*[36] also reported the presence of a crossover from elastic to plastic creep around the peak, although they reported positive μ using the $U(J) = U(J_{c0}/J)^{\mu}$ relation.

IV. CONCLUSION

We have measured the magnetization relaxation properties in OCMG-processed $NdBa_2Cu_3O_{7-\delta}$ bulk superconductors in a high-temperature region ($T \geqslant 77$ K). It is found that $Nd_4Ba_2Cu_2O_{10}$ (Nd422) inclusions are mainly effective in enhancing J_{net} without increasing the normalized relaxation rate $S(\equiv -d \ln M/d \ln t)$ at low fields [b_{irr} ($\equiv \mu_0 H_a / B_{irr}$) $\lesssim 0.1$] and high fields ($b_{irr} \gtrsim 0.4$). In addition, Nd422 refinement enhances J_{net} without increasing S, suggesting Nd422 inclusions are effective pinning centers in the fields studied here. A suppression of S is observed for all the Nd-based samples in an intermediate-field region ($0.1 \lesssim b_{irr} \lesssim 0.4$) at 77 K. The suppression is not observed when the peak in J is absent, i.e., either in melt-processed $YbBa_2Cu_3O_{7-\delta}$ bulk superconductor at 77 K or in OCMG processed Nd123 at $T = 90$ K. This implies that the peak in J is closely correlated with low T_c Nd123*ss*, which is believed to be the origin of the peak effect observed at $T \leqslant 88$ K.

ACKNOWLEDGMENTS

This work was supported by the New Energy and Industrial Technology Development Organization (NEDO) as Collaborative Research and Development of Fundamental Technologies for Superconductivity Applications under the New Sunshine Program administered by the Agency of Industrial Science and Technology (AIST) of the Ministry of International Trade and Industry (MITI) of Japan. The authors would like to thank Dr. H. S. Chauhan, Dr. H. Kojo, and K Sawada for the samples. Thanks are also due to Dr. M. R. Koblischka and K. Ogasawara for helpful discussion.

[1] G. Blatter, M.V. Feigel'man, V.B. Geshkenbein, A.I. Larkin, and V.M. Vinokur, Rev. Mod. Phys. **66**, 1125 (1994).
[2] Y. Yeshurun, A.P. Malozemoff, and A. Shaulov, Rev. Mod. Phys. **68**, 911 (1996).
[3] M.P. Maley, J.O. Wills, H. Lessure, and M.E. McHenry, Phys. Rev. B **42**, 2639 (1990); P.J. Kung, M.P. Maley, M.E. McHenry, J.O. Willis, J.Y. Coulter, M. Murakami, and S. Tanaka, *ibid.* **46**, 6427 (1992); P.J. Kung, M.P. Maley, M.E. McHenry, J.O. Willis, M. Murakami, and S. Tanaka, *ibid.* **48**, 13 922 (1993).
[4] For example, N. Chikumoto, M. Konczykowski, N. Motohira, and A.P. Molozemoff, Phys. Rev. Lett. **69**, 1260 (1992).
[5] M. Murakami, K. Yamaguchi, H. Fujimoto, N. Nakamura, T. Taguchi, N. Koshizuka, and S. Tanaka, Cryogenics **32**, 930 (1992).
[6] S.I. Yoo, N. Sakai, H. Takaichi, T. Higuchi, and M. Murakami, Appl. Phys. Lett. **65**, 633 (1994).
[7] M. Murakami, S.I. Yoo, T. Higuchi, N. Sakai, J. Weltz, N. Koshizuka, and S. Tanaka, Jpn. J. Appl. Phys., Part 2 **33**, L715 (1994); M. Murakami, S.I. Yoo, T. Higuchi, N. Sakai, M. Watahiki, N. Koshizuka, and S. Tanaka, Physica C **235-240**, 2781 (1994).
[8] M.R. Koblischka, A.J.J. van Dalen, T. Higuchi, S.I. Yoo, and M. Murakami, Phys. Rev. B **58**, 2863 (1998).
[9] T. Mochida, N. Chikumoto, and M. Murakami, Phys. Rev. B **62**, 1350 (2000).
[10] K. Sawada, S. I. Yoo, N. Sakai, T. Higuchi, and M. Murakmi, *4th Euro Ceramics*, edited by A. Barone, D. Fiorani, and A. Tampieri (Gruppo Editoriale Faenza Editrice, Faenza, 1995), Vol. 6, p. 293.
[11] H. Kojo, S.I. Yoo, N. Sakai, and M. Murakami, Superlattices Microstruct. **21**, 37 (1997).
[12] H.S. Chauhan and M. Murakami, Mater. Sci. Eng., B **56**, 48 (1999).
[13] T. Mochida, M. Takahashi, S. Goshima, N. Sakai, S.I. Yoo, and M. Murakami, Superlattices Microstruct. **21** Suppl. A, 37 (1997).
[14] T. Mochida, N. Sakai, S. I. Yoo, and M. Murakami, Physica C (to be published).
[15] J.R. Thompson, Y.R. Sun, and F. Holozberg, Phys. Rev. B **44**, 458 (1991); J.R. Thompson, Yang Ren Sun, L. Civale, A.P. Malozemoff, M.W. McElfresh, A.D. Marwick, and F. Holtzberg, *ibid.* **47**, 14 440 (1993); J.R. Thompson, Y.R. Sun, D.K. Christen, L. Civale, A.D. Marwick, and F. Holtzberg, *ibid.* **49**, 13 287 (1994).
[16] L. Civale, M.W. McElfresh, A.D. Marwick, F. Holtzverg, C. Feild, J.R. Thompson, and D.K. Christen, Phys. Rev. B **43**, 13 732 (1991).
[17] L. Civale, L. Krusin-Elbaum, J.R. Thompson, and F. Holtzberg, Phys. Rev. B **50**, 7188 (1994).
[18] A.J.J. van Dalen, M.R. Koblischka, H. Kojo, K. Sawada, T. Higuchi, and M. Murakami, Supercond. Sci. Technol. **9**, 659 (1996).
[19] B.H.P. Weisinger, F.M. Sauerzopf, and H.W. Weber, Physica C **203**, 121 (1992).
[20] S. Kirkpatrick, Rev. Mod. Phys. **45**, 574 (1973); Kari Harkone, Ilkka Tittonen, Jan Westerholm, and Kari Ullakko, Phys. Rev. B **39**, 7251 (1989).
[21] T. Higuchi, S.I. Yoo, and M. Murakami, Phys. Rev. B **59**, 1514 (1999).

[22] M.R. Koblischka, M. Muralidhar, T. Higuchi, K. Waki, N. Chikumoto, and M. Murakami, Supercond. Sci. Technol. **12**, 288 (1999).
[23] M. Muralidhar, M.R. Koblischka, J. Jirsa, and M. Murakami, Phys. Rev. B **62**, 13 911 (2000).
[24] B. Martinez, X. Obradors, A. Gou, V. Gomis, S. Pinol, J. Fontcuberta, and H. Van Tol, Phys. Rev. B **53**, 2797 (1996).
[25] M.R. Koblischka, A.J.J. van Dalen, T. Higuchi, K. Sawada, S.I. Yoo, and M. Murakami, Phys. Rev. B **54**, R6893 (1996).
[26] H.G. Schnack, R. Griessen, J.G. Lensink, and H.H. Wen, Phys. Rev. B **48**, 13 178 (1993); A.J.J. van Dalen, M.R. Koblischka, R. Griesen, M. Jirsa, and G. Ravi Kumar, Physica C **250**, 265 (1995).
[27] V.B. Geshkenbein and A.I. Larkin, Zh. Éksp. Teor. Fiz. **95**, 1108 (1989) [Sov. Phys. JETP **68**, 639 (1989)].
[28] L. Burlachkov, D. Giller, and R. Prozorov, Phys. Rev. B **58**, 15 067 (1998).
[29] M.V. Feigel'man, V.B. Geshkenbein, A.I. Larkin, and V.M. Vinokur, Phys. Rev. Lett. **63**, 2303 (1989); M.V. Feigel'man and V.M. Vinokur, Phys. Rev. B **41**, 8986 (1990); M.V. Feigel'man, V.B. Geshkenbein, and V.M. Vinokur, *ibid.* **43**, 6263 (1991).
[30] M.P.A. Fisher, Phys. Rev. Lett. **62**, 1415 (1989); D.S. Fisher, M.P.A. Fisher, and D.A. Huse, Phys. Rev. B **43**, 130 (1991).
[31] V.M. Vinokur, P.H. Kes, and A.E. Koshelev, Physica C **248**, 179 (1995).
[32] H. Küpfer, S.N. Gordeev, W. Jahn, R. Kresse, R. Meier-Hirmer, T. Wolf, A.A. Zhukov, K. Salama, and D. Lee, Phys. Rev. B **50**, 7016 (1994).
[33] Y. Kodama, K. Oka, Y. Yamaguchi, Y. Nishihara, and K. Kajimura, Phys. Rev. B **56**, 6265 (1997).
[34] R. Griessen, A.F.Th. Hoekstra, H.H. Wen, G. Doornbos, and H.G. Schnack, Physica C **282-287**, 347 (1997); H.H. Wen and Z. Zhao, Appl. Phys. Lett. **68**, 856 (1996).
[35] P.W. Anderson, Phys. Rev. Lett. **9**, 309 (1962); P.W. Anderson and Y.B. Kim, Rev. Mod. Phys. **36**, 39 (1964).
[36] Y. Abulafia, A. Shaulov, Y. Wolfus, R. Prozorov, L. Burlachkov, Y. Yeshurun, D. Majer, E. Zeldov, V.B. Geshkenbein, and V.M. Vinokur, Phys. Rev. Lett. **77**, 1596 (1996).